POLITECNICO DI TORINO
Repository ISTITUZIONALE

Little effect of further aging on soil-weathered plastics

Original
Little effect of further aging on soil-weathered plastics / Forsyth, H., Gnoffo, C., Stoll, R., Van Der Zee, M., Frache, A., Bigalke, M.. - In: SCIENTIFIC REPORTS. - ISSN 2045-2322. - 16:(2026), pp. 1-14.

Availability:
This version is available at: 11583/3017622 since: 2026-11-06T12:02:18Z

Publisher:
Springer Nature

Published
DOI:

Terms of use:

This article is made available under terms and conditions as specified in the corresponding bibliographic description in the repository

Publisher copyright

(Article begins on next page)

26 November 2026

scientific reports

Check for updates

OPEN

Little effect of further aging on soil-weathered plastics

Hannah Forsyth[1], Chiara Gnoffo[2], Rebecca Stoll[1], Maarten van der Zee[3], Alberto Frache[2] & Moritz Bigalke[1]✉

Plastic waste accumulates in soils, impacting structure, biota, and ecosystem functioning. Understanding the persistence and aging of plastics in soil is therefore important. However, aging occurs over timescales which cannot be covered in conventional experiments. Many studies therefore focus on simulated weathering of pristine polymers over short timescales, but these experiments do not consider potentially different aging behaviour after extended environmental exposure. To address this, we investigated the continued aging of naturally weathered macroplastics sampled from agricultural soils by reburying them under field conditions for 19 months and comparing properties before and after. Samples of polyethylene, polypropylene, polystyrene, and polyethylene terepthalate were analysed for chemical structure, surface oxidation (carbonyl index), crystallinity, molecular weight, thermal stability, and surface morphology. All samples showed signs of oxidative aging and aging-related surface alterations before and after reburial. After reburial, most samples had little to no change in carbonyl index, with several showing significant decreases, likely due to loss of highly oxidised surface layers through fragmentation. Crystallinity, thermal stability, and molecular weight remained largely unchanged. Overall, our results suggest that the further aging of weathered polymers does not follow the same trajectory as the initial aging and that conventional plastics degrade very slowly in soil.

Keywords Macroplastic, Soil pollution, Microplastic, Plastic pollution, Plastic degradation, Fragmentation

Abbreviations

AFM	Atomic force microscopy
ATR	Attenuated total reflectance
CI	Carbonyl index
CSS	Case study sites
CT	Computed tomography (µ-CT, micro-computed tomography)
DSC	Differential scanning calorimetry
ESEM	Environmental scanning electron microscopy
GPC	Gel permeation chromatography
HFIP	Hexafluoroisopropanol
KTFA	Potassium trifluoroacetate
MaP	Macroplastic
MINAGRIS	MIcro- and NAno-plastics in agricultural soils (EU Horizon 2020 funded project)
Mn	Number-average molecular mass
MPs	Microplastics
Mw	Weight-average molecular mass
NPs	Nanoplastics
PDI	Polydispersity index
PE	Polyethylene
PET	Polyethylene terephthalate
PMMA	Poly(methyl methacrylate)
PP	Polypropylene
PS	Polystyrene
PTFE	Polytetrafluoroethylene

[1]Institute of Applied Geosciences, Technical University of Darmstadt, Schnittspahnstr. 9, 64287 Darmstadt, Germany. [2]Department of Applied Science and Technology, Polytechnic of Turin, Viale Teresa Michel 5, Alessandria, Italy. [3]Wageningen Food & Biobased Research, Wageningen University & Research, Bornse Weilanden 9, 6708 WG Wageningen, The Netherlands. ✉email: moritz.bigalke@tu-darmstadt.de

PU	Polyurethane
PVC	Polyvinyl chloride
SAUB	Standard area under band
SD	Standard deviation
SEM	Scanning electron microscopy
TE-MCT	Thermoelectrically cooled - mercury cadmium telluride (FTIR detector)
TGA	Thermogravimetric analysis
TIC	Total inorganic carbon
TOC	Total organic carbon
UV	Ultraviolet (light)

Plastic waste has become ubiquitous in our society. 4900 Mt, representing 60% of all plastics ever produced, has been estimated to be discarded between 1950 and 2015[1]. Much of the plastic which is disposed ends up in soils. This can take the form of plastics released by littering[2,3], atmospheric deposition[4], and road runoff[5,6]. Plastic is also used extensively in agriculture, for example in mulch films[7,8], clips, nets, seedling trays[9], addition of sewage sludge[10] or compost[11], and fertiliser or seed coatings. The major plastic types used in agriculture are polypropylene (PP) and polyethylene (PE), mostly used in films, and polystyrene (PS), found in twine and nets[9]. Additionally, polyethylene terephthalate (PET), poly vinyl chloride (PVC), and polyurethane (PU) make up a large part of plastics disposed in the environment[12]. Macroplastics (MaPs), defined as particles >5 mm in size, can break down into microplastics (MPs, 1 µm – 5 mm) and nanoplastics (NPs, <1 µm) as they age, and are weathered in the natural environment.

Various physicochemical processes contribute to the aging of conventional plastics in soil, including photodegradation (relevant on the soil surface before complete burial), thermal degradation, hydrolysis, and biodegradation[13–17]. Polymers with a C-C backbone, such as PE, PP, and PS, are challenging to degrade, while polymers such as PET and PU which contain heteroatoms in their backbone are slightly more susceptible to hydrolysis and biodegradation[12,18]. Furthermore, various physical fragmentation processes can occur through biofragmentation, abrasion, mechanical stress, and freeze-thaw processes[13,14,19]. These processes are often studied under laboratory conditions using pristine plastics[20–24]. Previous work on simulated polymer weathering has found increases in surface oxidation and carbonyl index (CI), increases in crystallinity through preferential degradation of amorphous regions, changes in polymer chain length, increases in surface roughness, and leaching of additives, among other changes[20,25–28]. In soil specifically, reports vary from limited changes in CIs and crystallinity of conventional polymers in soil incubations up to 1 year[29], to increases in CI and surface roughness during soil burial[22]. However, the controlled experimental conditions employed in most studies cannot fully capture the heterogeneity in conditions found when exposed to environmental aging, for example temperature, moisture, humidity, soil organisms, and plants. Therefore, knowledge about the aging of conventional plastics in natural environmental conditions is still limited[29].

Investigating the long-term degradation of plastics in the environment presents a challenge, as the very slow degradation means that pristine polymers must be exposed to environmental conditions for potentially centuries or millennia to observe the full degradation[30,31], which is not feasible in experimental timescales. This is why many studies focus on simulated weathering of pristine polymers over short timescales. Some recent studies have used pristine materials buried in soil over 1 or 2 years to study early-stage aging[29,32]. However, as plastic properties change over aging[33,34], the processes and the rate of aging may also change. This is why studying the later stages of plastic aging is important in order to understand the full aging process and assess the persistence of plastics in the environment. An alternative approach is the use of naturally weathered plastics, which represent environmentally relevant materials that have already undergone long-term aging[35], potentially allowing the later stages of degradation to be investigated. Until now, naturally weathered polymers found in soil have been characterised for aging-related properties[35,36], but there is little knowledge about the continued aging of these polymers.

To close this information gap, we aimed to (1) determine the properties of naturally weathered MaPs found buried in soil, (2) investigate the surface aging of these particles upon reburial in soil under environmental field conditions for 19 months, and (3) examine changes in bulk properties including crystallinity, thermal stability, and molecular weight of the plastics after reburial. We focus on multiple polymer types (PE, PP, PS, and PET), including films, fibres, and rigid particles originating from real consumer applications rather than pristine materials. Emphasis was placed on MaPs, as these represent the precursor stage from which most MPs and NPs are generated. However, unlike for pristine plastics, the initial condition and exposure history of the naturally weathered plastics studied here are unknown. This introduces a higher uncertainty through the greater heterogeneity of the materials and the unknown initial conditions, but presents an opportunity to understand the later stages of aging in a considerable timeframe.

Materials and methods

Plastic materials and burial conditions

A total of 29 MaP particles were selected for the aging experiment. The particles analysed here were provided by the MINAGRIS project, which monitors 11 case study sites across Europe for MaPs, MPs and NPs. Each case study site comprises 2 fields from 11 farms distributed across the case study country. In each of these fields, the sampling area was defined as 400 m^2, avoiding field edges and uncultivated areas. In each sampling area, 4 areas of 1 m^2 arranged diagonally across the field were sampled to 10 cm and manually searched for MaPs, providing samples which were analysed as part of a larger dataset[37]. These samples were cleaned by shaking with water for 30 min and repeating until the water ran clear. From these, the particles to be used for this study were then selected based on covering a range of polymer types (PE, PP, PS, PET) and particle shapes (rigid fragments, films,

Sample	Shape	CI change	Crystallinity change(%)	TGA T_{PEAK} change (°C)	Mw (% change)	Optical Microscopy /SEM
PE-1	F	+0.05	NA	NA	NA	NA
PE-2	F	−0.06	−1.1	+1.7	NA	No change
PE-3	R	**−0.20**	0.0	−0.9	NA	NA
PE-4	R	**−0.23**	−1.3	−1.3	NA	No change
PE-5	R	**−0.18**	+0.5	+1.7	NA	NA
PE-6	R	**−0.19**	+0.1	+3.2	NA	NA
PE-7	F	**−0.26**	NA	NA	NA	NA
PE-8	F	**−0.43**	+0.9	**−10.3**	NA	NA
PE-9	F	−0.04	NA	NA	NA	NA
PE-10	R	+0.11	NA	NA	NA	NA
PP-1	R	−0.10	NA	NA	NA	NA
PP-2	R	−0.12	NA	NA	NA	NA
PP-3	R	**−0.56**	+3.9	**+25.7**	NA	No change
PP-4	R	**−0.23**	+2.2	+0.8	NA	NA
PP-5	R	−0.06	−0.7	−0.2	NA	No change
PS-1	R	**−1.98**	NA	NA	+1.2	NA
PS-2	R	**−0.93**	NA	NA	**−4.3**	No change
PS-3	R	−0.33	NA	NA	−0.7	NA
PS-4	R	−0.31	NA	NA	−2.6	NA
PS-5	R	**−1.24**	NA	NA	−0.7	NA
PS-6	R	−0.64	+0.4	+1.6	−2.6	No change
PS-7	R	+0.02	NA	NA	−1.2	NA
PS-8	R	+0.36	−1.2	**−11.9**	**−3.0**	NA
PET-1	T	NA	NA	NA	+0.9	NA
PET-2	T	NA	+2.6	+1.1	−1.4	NA
PET-3	T	NA	NA	NA	−0.4	NA
PET-4	T	NA	0.0	**+19.5**	+1.6	No change
PET-5	F	NA	−2.9	−1.7	−1.0	NA
PET-6	R	NA	NA	NA	**+4.2**	No change

Table 1. Summarised changes in properties (after - before) for the analysed samples. Values in bold either are statistically significant (for CI, $p < 0.05$) or above analytical variability (for crystallinity, TGA T_{PEAK}, and Mw change, where insufficient replicates were available to perform statistical testing). For shape, F = film, R = rigid, T = twine/fibre.

fibres), as well as ensuring an initial particle mass sufficient to be analysed by all the techniques listed below. An overview of the selected samples is shown in Table 1.

The selected particles were halved by cutting with scissors or a saw for more rigid particles (Fig. SI 1-4). One half of each particle was buried for 581 days (19 months, approx. 1.6 years) at a the edge of a corn field at a field study site near Dijon, France (47° 14' 05.0" N, 5° 6' 34.8" E), at a depth of ~10 cm. Monthly climatic data from Météo-France is included in Fig. SI 5[38]. All plastic pieces were buried at the same site to ensure comparable aging conditions during the reburial period. The particles were placed in a stainless-steel mesh box (mesh size = 12 mm) to ensure contact with soil, water, soil organisms, and plants while also enabling the samples to be recovered easily after the soil burial time. The samples were buried in summer and retrieved in winter. The second halves were kept as unexposed controls at room temperature in the dark for the experiment duration. Minor changes during storage cannot be completely excluded, but thermal oxidation of polyolefins is strongly temperature-dependent and has been reported to be negligible even at 60°C[39,40]. Therefore, oxidation during storage at ambient temperature is expected to be minimal and unlikely to contribute to changes in properties. Thus, for each sample, one "before" (control) and one "after" (exposed) particle were available for comparison. This approach was adopted to ensure sufficient material was available for comparison of both surface and bulk properties, and it was assumed that there was no systematic difference between the two halves. The samples were recovered from the field by manually searching through the soil inside the stainless steel mesh box. After recovery, particles were cleaned of adhering soil material following a procedure from Klaus et al.[41]. This cleaning protocol was applied to all "before" and "after" samples. In short, residues were first rinsed off with MilliQ water, particles were dried at 40 °C, then treated with a 0.1 M tetrasodium pyrophosphate solution ($Na_4P_2O_7$, Carl Roth, Germany), combined with shaking and ultrasonic treatment. This process was repeated for larger or fibrous samples until no visible residues remained, and samples were finally rinsed with MilliQ water and dried at 40 °C. For the soil, soil texture was determined according to DIN 18,123, total inorganic and organic carbon (TIC and TOC) were determined by TOC/TIC analysis (LiquiTOC II, Elementar, Langenselbold,

Germany), and soil pH was determined in a 1:2 soil-to-water suspension. The soil details were as follows: clay/silt/sand = 19.0/70.0/11.0% (silt loam), total organic C = 16.1 g kg^{-1}, total inorganic C = 6.4 g kg^{-1}, pH = 8.02.

ATR-FTIR analysis

The sample particles were analysed for their chemical composition using attenuated total reflectance – fourier transform infrared spectroscopy (ATR-FTIR, Lumos II, Bruker Corporation, Billerica, MA, USA) with a mercury-cadmium-telluride (TE-MCT) single-element detector. Each scan was repeated 32 times, and each particle was measured at 5 different points on each side, providing 10 measurements per sample half in order to compensate for surface variability. Further evaluation of spectra was performed in R Version 4.4.2[42]. Spectra underwent baseline correction using the "peakDetection" method in the "baseline" package[43], followed by normalisation to the intensity of the highest absorption band. Changes in the spectra were qualitatively analysed. For the fibrous PET samples, 15 measurements per side were carried out under a higher pressure between the crystal and the sample. Then, any spectra with an intensity less than 70% of the highest intensity spectrum measured were not analysed further, as they were deemed to have insufficient contact with the sample. This was because there was air between the fibres and much of what was being measured was air. This led to 2–13 spectra included for samples PET-1 to PET-5. Furthermore, a potential change in the chemical composition of plastics due to soil aging was examined using the Carbonyl Index (CI). The CI is used as a measure of polymer degradation, as it can describe the degree of surface oxidation[44].

For PP and PE, CI was calculated using the standard area under band (SAUB) method (Eq. 1)[45]. For PS, CI was calculated using Eq. 2[20,46]. However, for PET, CI was not calculated, as PET contains indigenous carbonyl groups and changes are more challenging to detect.

$$CI_{SAUB} = \frac{Area\ under\ band\ 1850 - 1650\ cm^{-1}}{Area\ under\ band\ 1500 - 1420\ cm^{-1}} \tag{1}$$

$$CI_{PS} = \frac{Area\ under\ band\ 1650 - 1635 cm^{-1}}{Absorbance\ at\ 1452\ cm^{-1}} \tag{2}$$

The CI was calculated for each individual measurement on PE, PP, and PS samples. To test whether the differences between "before" and "after" means were statistically significant, one-sided Welch's two-sample t-tests were conducted (assuming unequal variances), where normality was checked with the Kolmogorov-Smirnov test. A significant difference was reported where $p < 0.05$. Effect sizes were calculated using Hedges' g, with the pooled standard deviation used for standardisation and a correction for small-sample bias.

For visualisation only, spectra were smoothed using Open Specy (Savitzky–Golay filter, polynomial order = 2, wavenumber window = 50 cm^{-1}) after baseline correction and normalisation[47], and an artefact from the FTIR-ATR measurements caused by gaseous CO_2 in the vicinity of the measurement was removed through an x-axis break between 2000 and 2600 cm^{-1} [48].

Surface roughness analysis

For analysis of the surface morphology, images of selected samples were taken with both an optical microscope (Axio Zoom, Zeiss, Oberkochen, Germany) and an environmental scanning electron microscope (ESEM, FEI Quanta 400, FEI, Thermo Fischer Scientific, Massachusetts, US). Due to instrument availability issues, two samples each of PE, PP, PS, and PET were chosen for the analysis to provide a representative subset of samples. From each selected sample, one piece from the "before" and one from the "after" half were cut and mounted on conductive carbon adhesive pads (12 mm diameter). Where possible, the pieces were taken from the cut edge where the original sample was divided, ensuring the same side was chosen for analysis to maximise the comparability of the selected sample areas. Each sample half was imaged with optical microscopy at ×5 magnification (overview) and at three points at ×11.2 magnification. For ESEM analysis, the samples were coated with a Pt/Pd alloy (80:20) with 5 nm thickness for conductivity. Imaging was carried out using an Everhart-Thornley detector with an acceleration voltage of 12.5 kV. For each sample half ("before" and "after"), images were taken at three positions at magnifications of ×500, ×2000, ×10,000, and ×30,000 at each position. To account for local variability in surface morphology, measurement areas were chosen to be representative and evenly distributed across the sample surface. Large or obvious features (e.g., scratches from wear or mechanical damage rather than environmental aging) were excluded. However, because naturally weathered plastics can have heterogeneous surface morphology, differences in morphology between the two halves cannot be completely excluded.

Image analysis was performed with Fiji ImageJ[49]. The processing approach is based on detecting the edges in the image and using these as an indication of the surface roughness. The method assumes that degradation leads to increased crystallisation, brittleness, and more edges due to cracking or surface break-off[44]. The mean intensity of the transformed image was used here as a semi-quantitative metric to compare surface morphology between samples. The processing steps were:

1. Noise reduction with a median filter (radius 2 pixels).
2. Edge detection using the "Find Edges" function, converting images to grayscale where smooth areas appear dark and edges bright.
3. Generation of a grayscale histogram for each of the 3 measurement spots at each scale.
4. Calculation of mean intensity and standard deviation across the 3 measurement spots for each magnification, where higher mean intensity indicated more edge area in the image and hence higher surface roughness.

A schematic representation of the processing steps is shown in Fig. SI 6.

To test for significant differences between "before" and "after" halves for each magnification, an unpaired Welch's 2-sample t-test was carried out, where significant differences were defined with $p < 0.05$.

Bulk properties analysis (DSC, TGA, GPC)

A subset of 14 samples was selected for the analysis of crystallinity, melting enthalpy, and thermal stability due to instrument availability. For determination of crystallinity and melting enthalpy, differential scanning calorimetry (DSC) characterisation (TA Instruments DSC Q20, New Castle, USA) was used. The thermal cycle (performed under nitrogen atmosphere) included a heating scan from 0 to 300 °C with a rate of 10 °C min^{-1}. Melting temperature T_M and melting enthalpy ΔH_M were determined, and crystallinity, χ was evaluated according to Eq. 3, where ΔH_M is the melting enthalpy and $\Delta H_{M,100\%}$ is the melting enthalpy of the 100% crystalline polymer; 293 J g^{-1} for PE[50], 135 J g^{-1} for PET[51], 207 J g^{-1} for PP[52], and 87 J g^{-1} for PS[53].

$$\chi = 100 \times \frac{\Delta H_M}{\Delta H_{M,100\%}} \tag{3}$$

Thermogravimetric analysis (TGA, Discovery TGA 5500, New Castle, USA) was conducted to determine thermal stability, from 50 °C to 700 °C in nitrogen atmosphere with a heating rate of 10 °C min^{-1}. The temperature at which the degradation was at its maximum (i.e. the temperature of the peak in derivative thermogravimetric analysis (DTG) thermogram) was evaluated (T_{PEAK}) and was interpreted here as a measure of the thermal stability of the sample.

Gel permeation chromatography (GPC) measurements (OmniSEC HP-SEC system provided with a Triple Detector Array incl. RALLS + LALLS, RI Detector and Viscometer, Malvern Panalytical, UK) were carried out only on PS and PET samples due to issues with solubility of PE and PP. PET samples were dissolved in hexafluoroisopropanol (HFIP) with 0.02 M potassium trifluoroacetate (KTFA) and columns used were a PSS PFG analytical linear M and a guard column, molecular range ~ 300–2.5×10^6 Da (poly methyl methacrylate (PMMA) in HFIP). For PS, samples were dissolved in chloroform ($CHCl_3$) and columns used were a TSK-gel GMHHrm-M and a guard column. Samples were dissolved overnight in 3 mL of the mobile phase at concentrations of 4–6 mg mL^{-1}, then filtered through 0.45 µm polytetrafluoroethylene (PTFE) syringe filters. Calibrations were performed with a PolyCAL PMMA standard (Viscotek, Mw = 49,367 Da, Đ = 1.02) for HFIP and a PolyCAL PS standard (Viscotek, Mw = 99,209 Da, Đ = 1.03) for $CHCl_3$. Each sample was measured in duplicate. Mn (number-average molecular weight, giving greater weight to low molecular mass molecules), Mw (weight-average molecular weight, giving greater weight to high molecular mass molecules), and polydispersity index (PDI, Mw ÷ Mn), describing the breadth of the molecular weight distribution, were determined.

Results

Surface chemical aging of naturally soil-weathered plastics

We analysed the FTIR spectra of all the samples in order to determine their surface chemical aging status. Overview images of all samples are available in Fig SI 1–4. In total, 10 samples of PE were investigated in this work, comprising 5 film fragments and 5 rigid fragments. To determine the initial condition of the plastics, we examined the FTIR spectra of the samples prior to reburial (Fig. SI 7). The samples before the reburial were consistent with samples originating from agricultural fields with an unknown environmental history. These samples show some minor deviations from literature-reported spectra of non-degraded PE[20,54]. As it is not possible here to compare with an unaged version of our polymers, we use spectra of non-degraded PE from the literature, labelled "Reference PE" in Fig. 1a. However, these are for qualitative comparison only, since the initial material is not identical to the naturally weathered samples investigated in this work. In the hydroxyl region (3000–3600 cm^{-1}), the spectra show negligible difference to the reference. Similarly, in the carbonyl region between 1650 and 1850 cm^{-1}, only minor peaks were observed in 3 of the samples, indicating minimal surface oxidation. Next, we compared the FTIR spectra before and after the reburial. Across all PE samples, only minor changes in the FTIR spectra could be observed before and after the reburial, as shown in the example in Fig. 1a. Across all the PE samples, there was a statistically significant decrease in CI after the reburial ($p = 0.039$, Hedges' $g = -0.82$ $n = 10$), indicating a decrease in surface oxidation during the experimental burial period (Fig. 2). Looking at the samples individually, eight samples had lower CI values after reburial, with differences ranging from 0.04 to 0.43, of which six were statistically significant ($p < 0.05$). Changes are summarised in Table 1. The slight increases in CI values in two samples after reburial were not statistically significant ($p > 0.05$). For PE samples, a larger initial CI before reburial correlated with a larger decrease in CI after the reburial.

Next, 5 samples of PP were investigated, all of which were rigid fragments. The FTIR spectra of the "before" halves of the PP samples (Fig. SI 7) showed clear signs of oxidative degradation compared to reference spectra of non-degraded PP (example in Fig. 1b)[20,54]. No clear new peak could be detected in the 3000–3600 cm^{-1} hydroxyl region, but a carbonyl band between 1650 and 1850 cm^{-1} is visible in three samples. For PP, across all samples, the CI decreased slightly in the "after" halves, indicating a decrease in surface oxidation during the burial period (Fig. 2). However, this decrease was not statistically significant across all the samples ($p = 0.063$, Hedges' $g = -1.04$, $n = 5$). The decreases in CI for the individual samples ranged from 0.10 to 0.56, two of which were statistically significant ($p < 0.05$). Similarly to the PE samples, the samples with significant differences also had high initial CI values in their "before" halves, suggesting that they were already more oxidised prior to the experiment.

The 8 PS samples in this work were all rigid fragments. Compared to reference spectra of non-degraded PS[20,54], the FTIR spectra of the "before" halves of the PS samples show signs of oxidative aging (Fig. 1c). In the hydroxyl region, no clear new peak could be observed, but a carbonyl band was observed higher in intensity than in non-degraded PS for the majority of the samples. However, the samples after the reburial did not show a visual

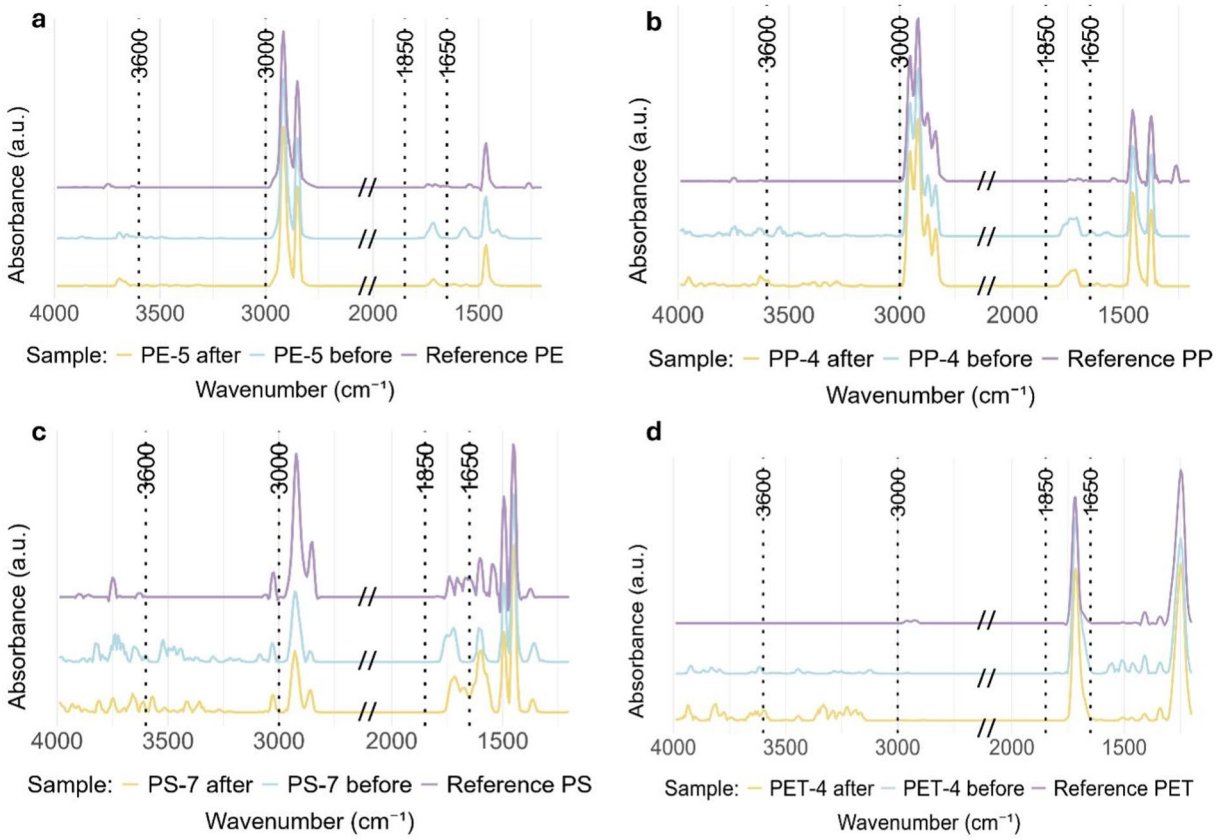

Fig. 1. FTIR analysis of samples recovered from agricultural fields and reburied for 1.6 years. Representative average FTIR spectra are shown for (**a**) PE-5, (**b**) PP-4, (**c**) PS-7, (**d**) PET-4. Marked wavenumber ranges denote ranges where emergence of new absorption bands has been observed after aging in the literature: 3000 to 3600 cm^{-1}, hydroxyl group, and 1650 to 1850 cm^{-1}, carbonyl group. "Reference" indicates a reference FTIR-ATR spectrum of an undegraded sample[54]. Note that an x-axis break was introduced between 2000 and 2600 cm^{-1} for visualisation, denoted by black slashes.

difference in the carbonyl peaks compared with before. Considering CIs, there was a statistically significant decrease in CI across all samples ($p = 0.019$, Hedges' $g = -1.14$, $n = 8$). In the individual samples, six exhibited lower CI values in the "after" halves, with decreases ranging from 0.31 to 1.98 (Fig. 2), of which three were statistically significant ($p < 0.05$). Two samples showed a small increase in CI after reburial, but these changes were not statistically significant. As observed for other polymers, samples with significant CI decreases also had high initial CI values in their "before" halves, indicating that they were already strongly oxidised prior to the experiment.

Finally, 6 samples of PET were investigated, of which 5 were fabric pieces and 1 was rigid. The FTIR spectra of the "before" halves of the PET samples (Fig. SI 7) show only minor deviations to reference spectra from the OpenSpecy database for non-degraded PET and others in the literature[47,54]. In the hydroxyl region, there was no clear increase in absorption intensity. The carbonyl region is difficult to assess due to the already strong characteristic absorption of PET. When comparing the FTIR spectra of the samples before and after the reburial, the same issue meant any differences were hard to detect (Fig. 1d). Accordingly, CI values were not determined for PET.

Surface analysis with optical microscopy and SEM

Surface imaging analysis was carried out on eight samples comprising two samples of each polymer type. Optical microscopy allowed identification of aging-related features on both sample halves, such as cracks, pits, and flaking. However, it was not possible to qualitatively assess any differences between the sample halves using this method. SEM images taken at 4 different magnifications were qualitatively and semi-quantitatively analysed to examine surface changes during reburial. For all samples, the "before" halves already showed clear signs of pre-existing environmental weathering, such as scratches, flaking, pitting, cracks, and surface irregularities. These features were likewise observed in the "after" halves. Some examples of aging-related structures detected are shown in Fig. 3. In most samples, it was not possible to qualitatively observe any changes between the two sample halves. However, in sample PP-3, the "before" half showed deeper, wider, and more undefined cracks compared to the "after" half, where the crack network appeared finer and more evenly distributed. SEM images of PP-3 at low magnification (× 50) showed that elevated regions surrounded by cracks were present in both halves but

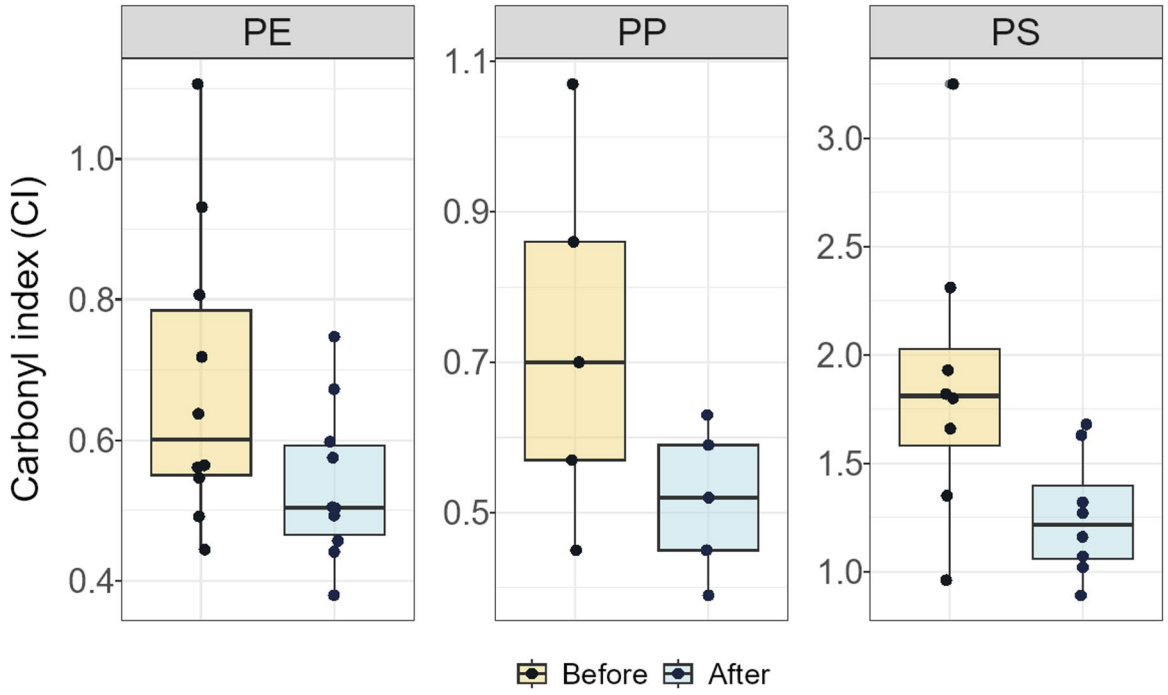

Fig. 2. Boxplot showing distribution of mean CIs calculated for each particle ($n = 10$ measurements per particle, 5 on each side) before and after the reburial. CIs of individual samples as well as the standard deviations, indicating within-sample variability, are shown in Fig. SI 8. Note that CI calculation is specific to the polymer type. Values for PE and PP were calculated using the same formula, whereas a different formula was applied for PS, so the resulting values cannot be directly compared.

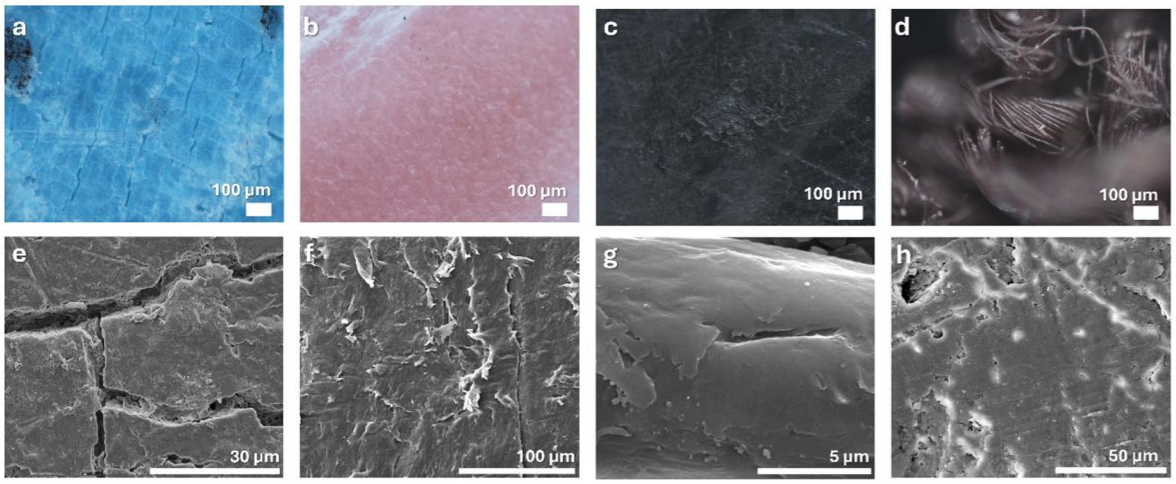

Fig. 3. Example optical microscopy (**a**–**d**) and SEM (**e**–**h**) images of samples, showing some of the features found in the samples. (**a**) PP-3 after reburial, showing deep, wide surface cracks and surface flaking. (**b**) PP-5 after reburial, showing an uneven surface with potential flaking. (**c**) PE-2 before reburial, showing surface pitting and flaking. (**d**) PET-4 after reburial, showing potential surface flaking. (**e**) PP-3 before reburial, showing deep, wide surface cracks and surface flaking. **f** PE-4 after reburial, showing an uneven surface with potential flaking. (**g**) PET-4 after reburial, showing surface flaking. (**h**) PS-6 after reburial, showing surface pitting and flaking.

occurred more frequently in the "after" half, suggesting that surface flaking may have occurred (Fig. SI 9). In the "before" half, the polymer within the cracks appeared to be flaking away from the surface (Fig. 3e). These results suggest that for all samples, much of the degradation occurred prior to the experimental period, with only limited additional change detectable during the reburial.

The semi-quantitative analysis involved image analysis to identify edges, which were used as a proxy for the surface roughness. The mean intensity of the histogram of the transformed image was used as a semi-quantitative measure of the area covered by edges in the image, with a higher value indicating increased surface roughness (Fig. SI 6). The edge analysis showed no significant difference in surface roughness after reburial, across all samples and magnifications ($p > 0.05$) (Fig. SI 10). The changes during reburial were challenging to assess due to pre-existing weathering structures rather than the development of new damage.

Bulk material properties

Thermal analysis (DSC and TGA) on a subset of 14 sample pairs before and after reburial indicated that polymer thermal properties remained largely unchanged during the reburial period. In the DSC results (Table 1, Table SI 1), melting temperature T_M remained stable across the samples, with an average change of $+0.4 \pm 1.2$ °C (mean ± SD). This was similar for the melting enthalpy ΔH_M and the crystallinity, which changed by $+0.37 \pm 3.37$ J g^{-1} and $+0.24 \pm 1.76$%, respectively (mean ± SD), indicating that the crystal structure of the polymers was largely unaffected by the reburial in soil. The low means reflect presence of both increases and decreases, whereas the high standard deviations indicate variability between samples, where individual samples differ substantially from each other. However, using a threshold of > 4% change in crystallinity to take into account errors related to peak integration, sample mass and instrument sensitivity, no individual samples exhibited crystallinity changes. Thermal stability assessed through TGA T_{PEAK} indicated an average change of $+2.1 \pm 9.8$ °C, again reflecting small changes inconsistent in direction and showing the overall thermal stability of the samples throughout the reburial period. Individually, just 2 samples showed large increases and 2 showed large decreases. Therefore, bulk thermal properties remained unchanged for the majority of samples during the reburial period.

GPC measurements were used to assess changes in polymer chain length during the experimental burial. As only PS and PET were soluble in the solvents required for the GPC analysis applied here, only these samples were analysed. During the analysis, the variability of Mn (difference between replicates expressed as %, average across all samples, mean ± SD) was 6.5 ± 3.4%, Mw variability was 1.6 ± 1.2%, and absolute difference in PDI between replicates was 0.11 ± 0.08. Across the PS samples, the majority of changes were small decreases and fall within the variability of the method, where on average, Mn changed by −7.0 ± 3.0%, Mw changed by −1.7 ± 1.7% and PDI change was +0.12 ± 0.05 (mean ± SD) after the reburial period. This suggests that no significant degradation or chain scission occurred. Means are influenced by a small number of larger changes in just 2 samples (Table 1). GPC results for PET similarly revealed negligible changes in molecular weight over the course of the burial (Mn: -0.3 ± 5.1%, Mw: +0.7 ± 2.1%, PDI: +0.03 ± 0.07, mean ± SD), with only one sample exhibiting a marginal increase in Mw (Table 1). Full results including Mn, Mw and PDI for all measured samples are available in Table SI 2. Overall, these results indicate that the molecular weight of PS and PET samples remained almost unchanged through the reburial.

Discussion

Surface aging of naturally soil-weathered plastics

As FTIR only penetrates 0.2–5 µm into the sample, this can only measure near-surface oxidation and does not indicate the oxidation of the bulk sample[55,56]. Before the reburial, many samples already showed signs of surface chemical oxidation. This is expected for weathered polymers found in the environment. They could be exposed to various weathering processes, including ultraviolet (UV) weathering while on the soil surface[15,20], thermal degradation[17], biodegradation[16,35], biofragmentation, freeze-thaw processes, and other anthropogenic physical soil disturbances such as ploughing which could generate surface scratches or abrasion[57]. Some samples are more weathered than others, which reflects their unknown background and the length of time they were buried in the soil. For PE, PP, and PS samples, peaks were present in some samples in the carbonyl region (1850–1650 cm^{-1}) which should not be present in pristine polymer, indicating surface oxidation[45,58]. None of the polymer types had distinct detectable peaks in the hydroxyl region (3600–3000 cm^{-1}), in contrast to other work which reported hydroxyl peaks alongside carbonyl peaks in naturally soil-weathered polymers for longer application times[35,59]. Artificially UV-weathered and naturally weathered riverine PE and PP also exhibit peaks in this region[20]. However, a study analysing agricultural plastic covers only detected carbonyl peaks, with no hydroxyl peaks observed[60]. These differing reports may arise from differences in the degree or mechanism of oxidation[26], as well as differences in the environmental conditions and plastic composition. Factors such as plastic colour, additives, thickness, soil conditions, moisture and temperature have been shown to influence the weathering behaviour and degradation mechanism, affecting which functional groups are detected in weathered plastics[61]. It also cannot be ruled out that hydroxyl peaks are present but below the resolution of the instrument. As the plastics investigated here have already undergone an unknown period of environmental exposure, and previous environmental conditions and initial state of the materials was not known, it is therefore not possible to determine the reason for the lack of a hydroxyl peak in the samples measured here.

After the reburial, the average CI across PE and PS samples exhibited a significant decrease, while PP samples did not decrease significantly despite individual samples showing decreases. However, this overall trend was not consistent across individual samples for all polymer types, where the majority of sample pairs did not show statistically significant changes. Despite this, the overarching trend indicates a small but significant decrease in CI across the analysed samples. In comparison to this study, changes reported in previous work are inconsistent, where pristine plastics rather than naturally weathered plastics are used to investigate aging. One study reports the appearance of a carbonyl peak in a PE fruit and vegetable bag after 77 days of incubation in soil followed by a disappearance of the peak after 185 days. Although the CIs are not calculated, this supports our result of decreasing CIs with increasing weathering time for some of our samples[62]. However, another study found an increase in CI after 8 weeks of soil incubation of pristine PE MPs in different soil types, with agricultural soil causing higher CI increase than grassland soil[63]. Other studies reported no changes in CI during soil burial. For

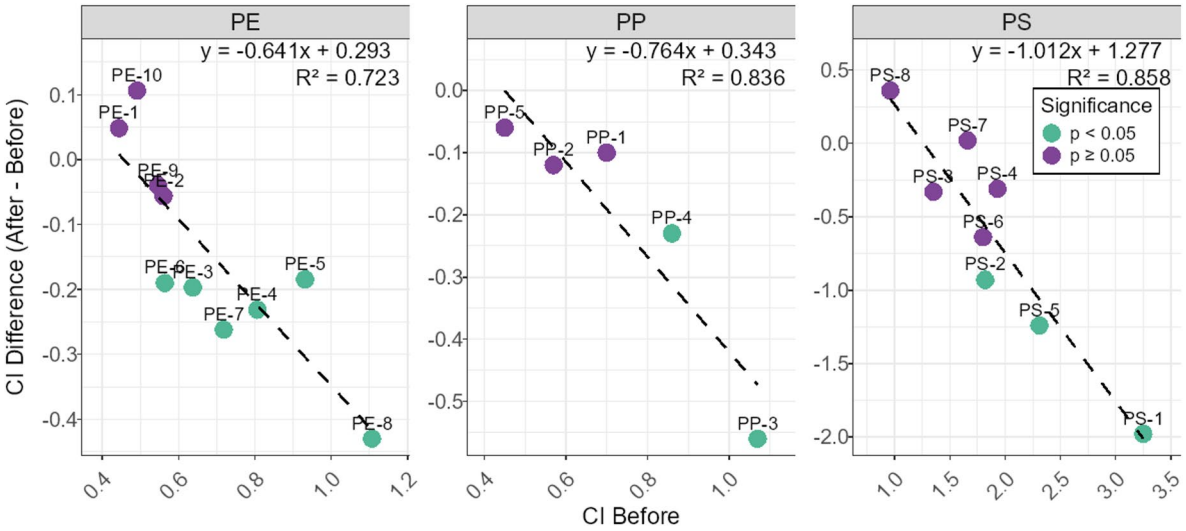

Fig. 4. Plots showing the CI before reburial vs. the difference between CI before and after the reburial (after – before) for all PE, PP, and PS samples. Samples with a significant difference are indicated in green. Points are labelled with their sample name.

instance, PE mulch films buried in soil for 125 days in laboratory experiments showed no significant difference in CI for both UV pre-aged and unaged PE films, although the CI of the UV-aged PE films was significantly higher than unaged samples[64]. In an outdoor pot experiment on aging of polymers in soil, there was similarly no significant effect of 1 year of soil burial on the carbonyl bands of PE[29]. For PS, samples of coffee cup lids were buried in soil for 2 years, but no changes in CI were observed during the burial time[32]. This could indicate an impact of soil type and particle size on the oxidation, as previously mentioned studies used different particle size ranges and did not compare different soil types. In comparison with these studies on pristine materials, the decrease in CI observed in our results could indicate that the continued aging of naturally weathered plastics in soil does not follow the same trajectory as pristine polymers.

In this study, a general trend could be observed where the samples with the highest initial CI showed the greatest decrease in CI for PE, PP, and PS, with a correlation between initial CI and the magnitude and direction of difference between the values before and after (Fig. 4). This suggests that higher surface oxidation led to a lower surface oxidation after the reburial. In contrast, previous work has reported increasing CI for increasing aging through accelerated weathering with UV or thermal treatment, for example with a CI of 0.18 vs. 2.26 before vs. after photo-oxidation of PP[20,45]. This could indicate that weathering of naturally weathered samples does not proceed in the same way as the simulated weathering of pristine samples. Indeed, it could be that after long-term weathering and storage in soil, CI does not continue to increase but reaches a limit, after which plastics may fragment. We hypothesise that the new surface post-fragmentation would then be less oxidatively weathered than the previous surface. This was also proposed by Syranidou et al.[58], who found that CI reaches a plateau (corresponding to saturation of the available surface) in PE and PP samples in a simulated marine environment, and that fragmentation occurs above a threshold CI and exposes less aged polymer beneath, where CI is higher for MPs formed from the initial material. Fragmentation could therefore explain the observation that samples with high initial CI exhibited the largest decrease in CI after reburial, as these samples were likely more susceptible to fragmentation. Alongside oxidative weathering, processes such as leaching of additives, freeze-thaw processes, and abrasion could also make plastic more brittle or cause surface fragmentation, limiting the CI increase. For example, sand abrasion has been shown to promote mechanical degradation of polymers[65]. However, while decreases in surface oxidation can be interpreted as evidence of fragmentation of oxidised surface layers, the occurrence of smaller fragments or microplastics was not assessed here. Future work should therefore aim to directly trace fragmentation processes and link these to surface oxidation changes to further assess the role of fragmentation in CI decreases. Alongside fragmentation, different degradation mechanisms (e.g. biotic vs. abiotic) could have an influence on the CIs observed in the present study. For instance, some studies report that the carbonyl group increases for abiotic degradation and decreases for biotic degradation[66–68]. This has been observed for PP, where carbonyl group increased up to 9 months in thermally pretreated polypropylene in soil, but after 12 months there was a decrease[68]. Recent work has also found that the CI of PE with an oxidised surface decreases after treatment with a yeast strain, attributing this to the higher bioavailability of carbonyl groups[69]. A biotic mechanism could therefore also contribute to the decrease in CI observed here. Furthermore, a decrease in CI could also be caused by leaching of low-molecular-weight oxidised degradation products from the surface[70,71]. In addition, the procedure for cleaning the particles may have contributed to the loss of loosely-attached oxidised fragments from the particle surfaces. This cleaning was necessary to remove adhering soil before ATR-FTIR and microscopy analysis, and was applied to all "before" and "after" samples to minimise systematic effects. However, we assume that the gentle cleaning just removed particles which were already

formed before due to aging-related crack formation. As the same procedure was applied to all samples, the influence of cleaning on the magnitude of the difference in CI between samples is expected to be limited.

Fragmentation as a potential mechanism for CI decrease is supported by the results of our surface analysis. All the samples, before and after aging, showed visible signs of surface aging, with surface cracking, pitting, flaking, and uneven texture in both optical microscopy and SEM images. Other studies of naturally weathered plastics recovered from soil likewise show aging signs such as cracking, pitting, and flaking [35,36]. While the surface edge analysis did not detect a significant difference in surface roughness between the samples before and after the reburial, there were some qualitative signs of changes in individual samples. For example, in some samples the cracking seemed to be more pronounced in the samples before the reburial. However, the method used here to investigate surface roughness has some limitations. The high magnification in SEM means that only part of the surface can be analysed, and one area of the surface could have a higher roughness than another area, leading to challenges in recording differences, or in failure to accurately represent a heterogeneous surface morphology. We observed that some areas of the samples were smoother than others. Furthermore, straight surface scratches, which are likely caused by external forces rather than by natural weathering, cannot be omitted in this method. In the present work, imaging was carried out in areas without obvious scratches where possible to avoid this issue. In contrast, in laboratory-scale or field-scale studies starting with an unaltered unaged polymer, or for biodegradable polymers, it is easier to detect surface morphological changes as the initial polymer generally has a smooth or well-defined surface, or degrades more quickly in the case of biodegradable polymers. For example, a study investigating the degradation of PE films in soil observed increased surface roughness after 100 days of soil burial in pot experiments, with appearance of cracks and pits[22]. When investigating environmentally aged polymers, SEM may be useful more as a descriptive technique showing the type of features detected than a technique to discover the changes in surface roughness parameters. Techniques such as atomic force microscopy (AFM) may be more suited to quantifying surface roughness[72,73], while micro-computed tomography (μ-CT) could be used to quantify bulk morphological changes[74].

Overall, our results highlight that the aging of naturally weathered polymers in soil does not proceed in the same way as studies with pristine polymers or with accelerated aging, with fragmentation potentially limiting increase in surface oxidation in MaPs, supported by SEM observations of sample surfaces. This indicates that CI should not be interpreted as a proxy for the age of polymers, but rather a snapshot of the surface oxidation at a particular timepoint. This is particularly important as a higher CI is often interpreted as higher surface aging in environmentally weathered plastic samples. For instance, CIs (SAUB method) of small PE MPs (2.58) and large PE MPs (0.70) at the sea surface were interpreted as being caused by higher surface oxidation of the smaller MPs which had been formed through fragmentation[75,76]. For artificially weathered polymers, this consideration may be less important, but for naturally weathered polymers, the impact of potential fragmentation may be increased and should be considered in the interpretation of CI. To obtain a more complete overview of the aging status of naturally weathered plastics, more aging parameters should be considered, including physical properties and surface morphology.

Bulk properties of naturally soil-weathered plastics upon further aging

In contrast to the surface aging, the majority of the samples had no measurable change in bulk properties during the reburial period. The results showed that melting temperature, melting enthalpy, and crystallinity remained stable on average, while the effects were inconsistent in direction. Note that for PS, crystallinity changes are less relevant as PS is amorphous[77], which we also observe with very low crystallinity for the PS samples. Crystallinity is usually expected to increase through aging, as amorphous polymer regions are more susceptible to degradation and once these are depleted, more highly crystalline regions remain[39]. However, in this work, no changes in crystallinity were observed. Accelerated weathering through UV exposure and humidity has led to changes in crystallinity of 16% in PE and 10% in PP in previous work[78], suggesting that processes occurring in soil are much slower and could be limited by lack of UV light. Similar to the DSC analysis results, the samples exhibited no change in thermal stability on average throughout the reburial period. T_{PEAK} could increase along with crystallinity increases which give higher thermal stability, or decrease, for example through chain scission[79]. Here, just two samples had a decrease in TGA T_{PEAK}, potentially related to chain scission. Increases were observed in two samples (one PP, one PET), but as no changes in crystallinity were observed, the mechanism behind this increase may be different.

For the PS and PET samples the average decrease in Mn and Mw fell within experimental variability, indicating no change in molecular weight during the experiment. However, two PS samples showed minor decreases in molecular weight, potentially indicating chain scission[80], while one PET sample showed a minor increase, which could potentially arise through crosslinking or leaching out of low molecular weight molecules formed by chain scission[81]. Molecular weight measured by GPC can decrease through chain scission, which is a direct result of aging[80]. Across all samples, the near-consistent decreases in Mn and increases in PDI could indicate very minor chain scission of low-molecular-weight chains leading to a broadening molecular weight distribution. Previous studies have observed molecular weight decreases by over 50% during accelerated weathering including UV exposure and mechanical stress[28,80], suggesting that for our samples, the weathering over 19 months in soil is much lower than that induced through accelerated weathering and UV aging.

Aging observations on naturally weathered polymers in soil

Overall, the majority of samples had little to no changes after the 19 month reburial period. This highlights the persistence of the conventional polymers investigated here in the soil environment. Measurable changes during reburial were more common at the surface than in the bulk polymer. The decreases in CI observed for several samples were not accompanied by consistent changes in crystallinity, molecular weight, or thermal stability. This suggests that changes in the surface layer did were generally not linked to changes to the bulk properties over the

19-month period. The conclusions are most robust for PE and PS, and slightly weaker for PP and PET through smaller sample numbers and lack of measurable CI for PET. Some individual samples showed changes in certain parameters but not in others, while few individual samples showed changes over multiple different measured parameters (Table 1). Sample PE-8 (a black mulch film) had a significant decrease in CI alongside a decrease in TGA T_{PEAK}, although no differences in crystallinity could be observed. This could reflect fragmentation or chain scission. Conversely, for sample PP-3, there was a significant decrease in CI alongside an increase in TGA T_{PEAK}, as well as qualitative observation of a more cracked surface in the "before" half. These results could indicate surface flaking leading to a lower CI with the release of fragmented layers potentially leaving behind a more thermally stable material. However, most other samples exhibiting significant decreases in CI did not exhibit a change in TGA T_{PEAK}, indicating that these do not always correlate. In sample PS-2, there was a significant decrease in CI alongside a decrease in molecular weight, which could indicate a combination of surface and bulk processes contributing to the aging. However, for this sample, no DSC and TGA data were available. For sample PS-8, the decrease in Mw was in line with the decrease in TGA T_{PEAK}, with both indicating chain scission, but there was no change in CI. Overall, these results show that that oxidation, crystallinity, thermal stability, and bulk molecular weight changes are not directly coupled here, and some parameters change in opposite directions for different samples. These heterogeneous changes highlight that aging does not impact all parameters at once and that the aging of polymers from different sources proceeds differently.

The observation of minor to no changes in most of the samples after the 19 months of reburial is consistent with the well-documented persistence of plastics in soil[31,57]. Previous field studies have reported the presence of plastics in soil more than 30 years after disposal, either in a relatively intact form or as MPs[35,82]. Plastics in soil will form MPs and NPs through fragmentation[81], as we also observed in the current study. In contrast to accelerated weathering experiments or studies investigating early-stage degradation of pristine polymers in soils, we did not observe systematically increasing CI, crystallinity, or related degradation indicators. Rather, we observed a range of different responses. Furthermore, the magnitude of changes observed here were much smaller or non-existent compared with aging induced through simulated UV exposure. Therefore, aging clearly takes place over a very long timescale in natural environments. Moreover, environmentally pre-aged polymers may not continue to follow the same degradation trajectory as pristine materials, and later stages of aging may involve different dominant mechanisms than initial oxidation and chain scission. For example, decreases in CI potentially caused through fragmentation processes may only become apparent after prolonged environmental exposure, which should be considered when interpreting CI of naturally weathered plastics. The effects of aging seem to also be sample-dependent and are likely influenced by additives in the original product such as anti-or pro-oxidants, flame retardants, and colourants[83–85], as well as intrinsic polymer properties such as chemical structure, crystallinity, and molecular weight[86]. Furthermore, the prior environmental exposure history of the sampled plastics is unknown and likely varies between samples. These compositional differences may partly explain the heterogeneous responses observed among samples. This shows the inherent challenge of investigating the continued degradation of naturally weathered plastics, as the starting points of aging and aging history are unknown. In this work, the number of samples analysed was limited due to the time and analytical effort of the measurements. Therefore, while observations were made here of heterogeneous changes in bulk properties and a relationship between high surface oxidation and fragmentation, these could also be influenced by the different extent in environmental exposure and initial material properties and may differ for samples with a different history. Nevertheless, naturally weathered plastics provide opportunity to investigate later stages of degradation, which cannot be studied with controlled aging of pristine polymers under environmentally relevant conditions without long-term exposure experiments over years to decades. Overall, as the combined load of plastics in soils can cause alterations to soil structure, biota, and biogeochemical processes, the persistence of plastics in soil and their continued accumulation may exacerbate these effects over time[87–89].

Conclusions

Overall, our findings show that for the naturally weathered macroplastics examined here, aging is very slow, and polymers are highly persistent despite previous environmental exposure history. Although the unknown history and initial condition of naturally weathered plastics introduces uncertainty, studying these materials is a valuable approach for understanding the long-term environmental aging of plastics under realistic conditions. The observed changes were heterogeneous and sample-dependent, reflecting the diverse origins of the materials and the wide range of polymer types with different additives and compositions present in the environment, as well as their differing environmental exposure histories. Across the samples, CI values generally decreased, crystallinity remained stable, and molecular weight and thermal stability remained stable overall, showing minimal individual increases and decreases depending on the sample. A trend was observed between initially high CI values and subsequent decreases in CI during the reburial period. Fragmentation was identified as a potential explanation for the observed decreases in CI, indicating that this process should be considered when interpreting CI values. This suggests that CI cannot be interpreted as an indicator of polymer age, rather as an indicator of current surface oxidation. Despite observation of surface flaking and pitting, no significant changes in surface roughness were detected using the applied SEM analysis method. Indeed, this work illustrated the difficulty of characterising surface morphological changes in environmentally pre-aged polymers, which arose from the challenge of ensuring the representativeness of individual images. Overall, the slow and heterogeneous changes in surface and bulk properties observed here limit mechanistic interpretation of aging processes, indicating that more sensitive, high-resolution approaches are needed to resolve processes occurring over shorter timescales. The findings suggest that later-stage aging is not directly comparable with earlier-stage simulated weathering of pristine polymers.

Data availability

The datasets generated and analysed during the current study are available in the Zenodo repository, https://doi.org/10.5281/zenodo.20306686.

Received: 11 August 2026; Accepted: 26 October 2026
Published online: 05 November 2026

References

1. Geyer, R., Jambeck, J. R. & Law, K. L. Production, use, and fate of all plastics ever made. *Sci. Adv.* **3**, e1700782 (2017).
2. Ledieu, L. et al. Amount, composition and sources of macrolitter from a highly frequented roadway. *Environ. Pollut*. **303**, 119145 (2022).
3. Pietz, O. et al. Macroplastic accumulation in roadside ditches of New York State's Finger Lakes region (USA) across land uses and the COVID-19 pandemic. *J. Environ. Manage.* **298**, 113524 (2021).
4. Allen, D. et al. Microplastics and nanoplastics in the marine-atmosphere environment. *Nat. Rev. Earth Environ.* **2022**, 1–13. https://doi.org/10.1038/s43017-022-00292-x (2022).
5. Knight, L. J., Parker-Jurd, F. N. F., Al-Sid-Cheikh, M. & Thompson, R. C. Tyre wear particles: An abundant yet widely unreported microplastic? *Environ. Sci. Pollut Res.* **27**, 18345–18354 (2020).
6. Sommer, F. et al. Tire Abrasion as a major source of microplastics in the environment. *Aerosol Air Qual. Res.* **18**, 2014–2028 (2018).
7. Kasirajan, S. & Ngouajio, M. Polyethylene and biodegradable mulches for agricultural applications: A review. *Agron. Sustain. Dev.* **32**, 501–529 (2012).
8. Steinmetz, Z. & Schröder, H. Plastic debris in plastic-mulched soil—a screening study from western Germany. *PeerJ* **10**, e13781 (2022).
9. Huerta Lwanga, E. H. et al. Review of microplastic sources, transport pathways and correlations with other soil stressors: A journey from agricultural sites into the environment. *Chem. Biol. Technol. Agric.* **9**, 20 (2022).
10. Corradini, F. et al. Evidence of microplastic accumulation in agricultural soils from sewage sludge disposal. *Sci. Total Environ.* **671**, 411–420 (2019).
11. Braun, M., Mail, M., Krupp, A. E. & Amelung, W. Microplastic contamination of soil: Are input pathways by compost overridden by littering? *Sci. Total Environ.* **855**, 158889 (2023).
12. Gewert, B., Plassmann, M., MacLeod, M. & M. & Pathways for degradation of plastic polymers floating in the marine environment. *Environ. Sci. Process. Impacts*. **17**, 1513–1521 (2015).
13. Ali, S. S. et al. Degradation of conventional plastic wastes in the environment: A review on current status of knowledge and future perspectives of disposal. *Sci. Total Environ.* **771**, 144719 (2021).
14. Astner, A. F. et al. Mechanical formation of micro- and nano-plastic materials for environmental studies in agricultural ecosystems. *Sci. Total Environ.* **685**, 1097–1106 (2019).
15. Cai, L., Wang, J., Peng, J., Wu, Z. & Tan, X. Observation of the degradation of three types of plastic pellets exposed to UV irradiation in three different environments. *Sci. Total Environ.* **628–629**, 740–747 (2018).
16. Muangchinda, C., Naloka, K. & Pinyakong, O. Enhanced soil biodegradation of low-density polyethylene (LDPE) by a synthetic bacterial consortium: Performance, mechanisms, and community dynamics. *Sci. Total Environ.* **996**, 180131 (2025).
17. Pielichowski, K., Njuguna, J. & Majka, T. M. *Thermal Degradation of Polymeric Materials* (Elsevier, 2022).
18. Krueger, M. C., Harms, H. & Schlosser, D. Prospects for microbiological solutions to environmental pollution with plastics. *Appl. Microbiol. Biotechnol.* **99**, 8857–8874 (2015).
19. Dawson, A. L. et al. Turning microplastics into nanoplastics through digestive fragmentation by Antarctic krill. *Nat. Commun.* **9**, 1001 (2018).
20. Campanale, C., Savino, I., Massarelli, C. & Uricchio, V. F. Fourier transform infrared spectroscopy to assess the degree of alteration of artificially aged and environmentally weathered microplastics. *Polymers* **15**, 911 (2023).
21. Chelliah, A., Subramaniam, M. & Gupta, R. G. Evaluation on the thermo-oxidative degradation of PET using prodegradant additives. *Indian J. Sci. Technol.* **10**, 1–5 (2017).
22. Huang, D. et al. Degradation of polyethylene plastic in soil and effects on microbial community composition. *J. Hazard. Mater.* **416**, 126173 (2021).
23. Miranda, M. N., Sampaio, M. J., Tavares, P. B., Silva, A. M. T. & Pereira, M. F. R. Aging assessment of microplastics (LDPE, PET and uPVC) under urban environment stressors. *Sci. Total Environ.* **796**, 148914 (2021).
24. Sun, Y. et al. Laboratory simulation of microplastics weathering and its adsorption behaviors in an aqueous environment: A systematic review. *Environ. Pollut*. **265**, 114864 (2020).
25. Ainali, N. M., Bikiaris, D. N. & Lambropoulou, D. A. Aging effects on low- and high-density polyethylene, polypropylene and polystyrene under UV irradiation: An insight into decomposition mechanism by Py-GC/MS for microplastic analysis. *J. Anal. Appl. Pyrol.* **158**, 105207 (2021).
26. Anshari, R., Tsuboi, M., Sato, H., Tashiro, K. & Ozaki, Y. Raman and ATR-FTIR unmask crystallinity changes and carboxylate group and vinyl group accumulation in natural weathering polypropylene microplastics. *Sci. Rep.* **15**, 2518 (2025).
27. Bonechi, P., Kandylioti, I., Cincinelli, A., Ionescu, I. A. & Psillakis, E. Linear relationship between carbonyl index of weathered microplastics with a CC backbone and solar light photodegradation kinetics of nicotine. *J. Photochem. Photobiol Chem.* **470**, 116609 (2026).
28. Meides, N. et al. Reconstructing the environmental degradation of polystyrene by accelerated weathering. *Environ. Sci. Technol.* **55**, 7930–7938 (2021).
29. Beltrán-Sanahuja, A., Benito-Kaesbach, A. & Sánchez-García, N. Sanz-Lázaro, C. Degradation of conventional and biobased plastics in soil under contrasting environmental conditions. *Sci. Total Environ.* **787**, 147678 (2021).
30. Albertsson, A. C. & Karlsson, S. The three stages in degradation of polymers—polyethylene as a model substance. *J. Appl. Polym. Sci.* **35**, 1289–1302 (1988).
31. Albertsson, A. C. Biodegradation of synthetic polymers. II. A limited microbial conversion of 14 C in polyethylene to $14CO_2$ by some soil fungi. *J. Appl. Polym. Sci.* **22**, 3419–3433 (1978).
32. Trusler, M. M., Kent, M. S., Lomax, B. H., Vane, C. H. & Cook, S. The use of ATR-FTIR to track the degradation of single-use polystyrene cup lids during 24 months of temperate outdoor exposure. *PLOS ONE*. **20**, e0330354 (2025).
33. Binda, G. et al. Microplastic aging processes: Environmental relevance and analytical implications. *TrAC Trends Anal. Chem.* **172**, 117566 (2024).
34. Alimi, O. S. et al. Effects of weathering on the properties and fate of secondary microplastics from a polystyrene single-use cup. *J. Hazard. Mater.* **131855** https://doi.org/10.1016/j.jhazmat.2023.131855 (2023).
35. Otake, Y., Kobayashi, T., Asabe, H., Murakami, N. & Ono, K. Biodegradation of low-density polyethylene, polystyrene, polyvinyl chloride, and urea formaldehyde resin buried under soil for over 32 years. *J. Appl. Polym. Sci.* **56**, 1789–1796 (1995).
36. Fernandes, E. M. S., de Souza, A. G., Barbosa, R. F. S. & Rosa, D. S. Municipal park grounds and microplastics contamination. *J. Polym. Environ.* **30**, 5202–5210 (2022).

37. Alaoui, A. *et al. MINAGRIS Monitoring Plan*. https://cordis.europa.eu/project/id/101000407/results (2022). https://doi.org/10.3030/101000407
38. Météo-France. Public data from Météo-France - Climate bulletins for metropolitan and overseas France - station Dijon–Longvic (21473001). https://donneespubliques.meteofrance.fr/?fond=produit&id_produit=129&id_rubrique=52.
39. Aniśko-Michalak, J. et al. Unveiling the effects of thermal aging on the oxidative stability of biobased low-density polyethylenes. *ACS Omega*. **10**, 25432–25450 (2025).
40. Yang, R., Liu, Y., Yu, J. & Wang, K. Thermal oxidation products and kinetics of polyethylene composites. *Polym. Degrad. Stab.* **91**, 1651–1657 (2006).
41. Klaus, J., Seeger, M., Bigalke, M. & Weber, C. J. Microplastics in vineyard soils: First insights from plastic-intensive viticulture systems. *Sci. Total Environ.* **947**, 174699 (2024).
42. R Core Team. *R: A Language and Environment for Statistical Computing* (R Foundation for Statistical Computing, 2024).
43. Liland, K. H. & Mevik, B. H. baseline: Baseline Correction of Spectra. 1.3-7 (2011). https://doi.org/10.32614/CRAN.package.baseline
44. Gomes, S., Fernandes, R., Waldman, W. R. & A. N. & How to measure polymer degradation? An analysis of authors' choices when calculating the carbonyl index. *Environ. Sci. Technol.* https://doi.org/10.1021/acs.est.3c10855 (2024).
45. Almond, J., Sugumaar, P., Wenzel, M. N., Hill, G. & Wallis, C. Determination of the carbonyl index of polyethylene and polypropylene using specified area under band methodology with ATR-FTIR spectroscopy. *E-Polym* **20**, 369–381 (2020).
46. Rodrigues, M. O. et al. Spatial and temporal distribution of microplastics in water and sediments of a freshwater system (Antuã River, Portugal). *Sci. Total Environ.* **633**, 1549–1559 (2018).
47. Cowger, W. et al. Microplastic spectral classification needs an open source community: Open Specy to the Rescue! *Anal. Chem.* **93**, 7543–7548 (2021).
48. Volkov, D. S., Rogova, O. B. & Proskurnin, M. A. Organic matter and mineral composition of silicate soils: FTIR comparison study by photoacoustic, diffuse reflectance, and attenuated total reflection modalities. *Agronomy* **11**, 1879 (2021).
49. Schindelin, J. et al. Fiji: an open-source platform for biological-image analysis. *Nat. Methods*. **9**, 676–682 (2012).
50. Bernagozzi, G., Arrigo, R. & Frache, A. High melt strength recycled high-density polyethylene: Evaluation of a novel route for targeting the polymer microstructure. *Polymers* **17**, 382 (2025).
51. Shieh, Y. T., Lin, Y. S., Twu, Y. K., Tsai, H. B. & Lin, R. H. Effect of crystallinity on enthalpy recovery peaks and cold-crystallization peaks in PET via TMDSC and DMA studies. *J. Appl. Polym. Sci.* **116**, 1334–1341 (2010).
52. Gnoffo, C., Arrigo, R., Sisani, M. & Frache, A. Elongational flow-induced microstructure evolutions in polypropylene/layered double hydroxides nanocomposites. *Polym. Compos.* **45**, 6606–6617 (2024).
53. Xu, H., Ince, B. S. & Cebe, P. Development of the crystallinity and rigid amorphous fraction in cold-crystallized isotactic polystyrene. *J. Polym. Sci. Part. B Polym. Phys.* **41**, 3026–3036 (2003).
54. Morgado, V., Gomes, L., Bettencourt da Silva, R. J. N. & Palma, C. Validated spreadsheet for the identification of PE, PET, PP and PS microplastics by micro-ATR-FTIR spectra with known uncertainty. *Talanta* **234**, 122624 (2021).
55. Foetisch, A., Filella, M., Watts, B., Bragoni, M. & Bigalke, M. After the sun: A nanoscale comparison of the surface chemical composition of UV and soil weathered plastics. *Microplast. Nanoplast.*. **3**, 18 (2023).
56. Wärnheim, A. et al. Depth-resolved FTIR-ATR imaging studies of coating degradation during accelerated and natural weatheringinfluence of biobased reactive diluents in polyester melamine coil coating. *ACS Omega*. **7**, 23842–23850 (2022).
57. Ghatge, S., Yang, Y., Ahn, J. H. & Hur, H. G. Biodegradation of polyethylene: A brief review. *Appl. Biol. Chem.* **2020 631**, 63, 1–14 (2020).
58. Syranidou, E. et al. Relationship between the carbonyl index (CI) and fragmentation of polyolefin plastics during aging. *Environ. Sci. Technol.* **57**, 8130–8138 (2023).
59. Yang, J. et al. Distribution and weathering characteristics of microplastics in paddy soils following long-term mulching: A field study in Southwest China. *Sci. Total Environ.* **858**, 159774 (2023).
60. Steinmetz, Z. et al. Are agricultural plastic covers a source of plastic debris in soil? A first screening study. *SOIL* **8**, 31–47 (2022).
61. Groß, M., Mail, M., Debastiani, R., Scherer, T. & Braun, M. Weathering of plastics in terrestrial environments. *TrAC Trends Anal. Chem.* **190**, 118281 (2025).
62. Huo, Y., Dijkstra, F. A., Possell, M., Dong, A. Z. & Singh, B. Degradation of conventional, biodegradable and oxo-degradable microplastics in a soil using a d13C technique. *Soil. Res.* **61**, 755–765 (2023).
63. Zhang, H. et al. Mechanism of polyethylene and biodegradable microplastic aging effects on soil organic carbon fractions in different land-use types. *Sci. Total Environ.* **912**, 168961 (2024).
64. La Mantia, F. P., Ascione, L., Mistretta, M. C., Rapisarda, M. & Rizzarelli, P. Comparative investigation on the soil burial degradation behaviour of polymer films for agriculture before and after photo-oxidation. *Polymers* **12**, 753 (2020).
65. Ziemann, S. et al. Novel release mechanism of microplastics and nanoplastics by environmentally relevant sand abrasion. *Environ. Sci. Technol.* **59**, 20684–20694 (2025).
66. Albertsson, A. & Karlsson, S. The influence of biotic and abiotic environments on the degradation of polyethylene. *Prog Polym. Sci.* **15**, 177–192 (1990).
67. Albertsson, A. C., Barenstedt, C., Karlsson, S. & Lindberg, T. Degradation product pattern and morphology changes as means to differentiate abiotically and biotically aged degradable polyethylene. *Polymer* **36**, 3075–3083 (1995).
68. Arkatkar, A., Arutchelvi, J., Bhaduri, S., Uppara, P. V. & Doble, M. Degradation of unpretreated and thermally pretreated polypropylene by soil consortia. *Int. Biodeterior. Biodegrad*. **63**, 106–111 (2009).
69. Buron-Moles, G. et al. Biodegradation of pre-treated low-density polyethylene (LDPE) by *Yarrowia lipolytica* determined by oxidation and molecular weight reduction. *Polym. Degrad. Stab.* **236**, 111292 (2025).
70. Gewert, B., Plassmann, M., Sandblom, O. & MacLeod, M. Identification of chain scission products released to water by plastic exposed to ultraviolet light. *Environ. Sci. Technol. Lett.* **5**, 272–276 (2018).
71. Biale, G. et al. Seeping plastics: Potentially harmful molecular fragments leaching out from microplastics during accelerated ageing in seawater. *Water Res.* **219**, 118521 (2022).
72. Joshi, G. et al. Unraveling the plastic degradation potentials of the plastisphere-associated marine bacterial consortium as a key player for the low-density polyethylene degradation. *J. Hazard. Mater.* **425**, 128005 (2022).
73. Khandare, S. D., Agrawal, D., Mehru, N. & Chaudhary, D. R. Marine bacterial based enzymatic degradation of low-density polyethylene (LDPE) plastic. *J. Environ. Chem. Eng.* **10**, 107437 (2022).
74. Groß, M. et al. Plastic fruit stickers in industrial compostingsurface and structural alterations revealed by electron microscopy and computed tomography. *Environ. Sci. Technol.* **58**, 7124–7132 (2024).
75. Celik, M. et al. Carbonyl index of miniaturized microplastics at the sea surface. *Mar. Pollut Bull.* **211**, 117376 (2025).
76. Celik, M., Nakano, H., Uchida, K., Isobe, A. & Arakawa, H. Comparative evaluation of the carbonyl index of microplastics around the Japan coast. *Mar. Pollut Bull.* **190**, 114818 (2023).
77. Sorolla-Rosario, D., Llorca-Porcel, J., Pérez-Martínez, M. & Lozano-Castelló, D. Bueno-López, A. Study of microplastics with semicrystalline and amorphous structure identification by TGA and DSC. *J. Environ. Chem. Eng.* **10**, 106886 (2022).
78. Hoseini, M., Stead, J. & Bond, T. Ranking the accelerated weathering of plastic polymers. *Environ. Sci. Process. Impacts*. **25**, 2081–2091 (2023).
79. Li, X. et al. Effects of short-term thermal oxidation on the mechanical and thermal behavior of PA6 liner material for type IV hydrogen storage cylinders. *RSC Adv.* **15**, 16375–16391 (2025).

80. Shen, Z., Lan, B. & Yang, Q. A new viewpoint on aging degradation of polystyrene: From the perspective of molecular weight. *Polymer* **288**, 126447 (2023).
81. Pfohl, P. et al. Environmental degradation and fragmentation of microplastics: Dependence on polymer type, humidity, UV dose and temperature. *Microplast. Nanoplast.* . **5**, 7 (2025).
82. Weber, C. J., Santowski, A. & Chifflard, P. Investigating the dispersal of macro- and microplastics on agricultural fields 30 years after sewage sludge application. *Sci. Rep.* **12**, 6401 (2022).
83. Hahladakis, J. N., Velis, C. A., Weber, R., Iacovidou, E. & Purnell, P. An overview of chemical additives present in plastics: Migration, release, fate and environmental impact during their use, disposal and recycling. *J. Hazard. Mater.* **344**, 179–199 (2018).
84. Monclús, L. et al. Mapping the chemical complexity of plastics. *Nature* **643**, 349–355 (2025).
85. Terzopoulou, Z., Wahbi, M., Kasmi, N., Papageorgiou, G. Z. & Bikiaris, D. N. Effect of additives on the thermal and thermo-oxidative stability of poly(ethylene furanoate) biobased polyester. *Thermochim Acta*. **686**, 178549 (2020).
86. Maddison, C., Sathish, C. I., Lakshmi, D., Wayne, O. & Palanisami, T. An advanced analytical approach to assess the long-term degradation of microplastics in the marine environment. *Npj Mater. Degrad.* **7**, 1–11 (2023).
87. Cramer, A., Benard, P., Zarebanadkouki, M., Kaestner, A. & Carminati, A. Microplastic induces soil water repellency and limits capillary flow. *Vadose Zone J.* **22**, e20215 (2023).
88. Dhevagi, P. et al. The crux of microplastics in soil - a review. *Int. J. Environ. Anal. Chem.* **0**, 1–33 (2022).
89. Lehmann, A., Leifheit, E. F., Gerdawischke, M. & Rillig, M. C. Microplastics have shape- and polymer-dependent effects on soil aggregation and organic matter loss – an experimental and meta-analytical approach. *Microplast. Nanoplast.*. **1**, 7 (2021).

Acknowledgements

This work is part of the MINAGRIS (MIcro- and Nanoplastics in AGRIcultural Soils) Project, which is funded by the European Union's Horizon 2020 Programme for research & innovation under Grant Agreement number: 101000407. We would like to acknowledge Kerstin Stricker for help in ESEM imaging, Collin Weber for support with µFTIR analysis, and Wouter Teunissen and Fresia Alvarado Chacon for GPC analysis. Thank you to Fabrice Martin and Abdelwahad Echairi from INRAE and Sayens for access to the burial site in Dijon, France.

Author contributions

HF: Conceptualisation, Methodology, Investigation, Validation, Formal analysis, Data curation, Writing—original draft, Visualisation. CG: Methodology, Investigation, Formal analysis, Writing—review and editing. RS: Methodology, Investigation, Formal analysis, Writing— review and editing. MvdZ Conceptualisation, Resources, Methodology, Funding acquisition, Writing—review and editing. AF: Conceptualisation, Resources, Methodology, Supervision, Project administration, Funding acquisition, Writing—review and editing. MB: Conceptualisation, Methodology, Resources, Writing—review and editing, Project administration, Funding acquisition, Supervision.

Funding

Open Access funding enabled and organized by Projekt DEAL. This work was funded through the MINAGRIS (MIcro- and Nanoplastics in AGRIcultural Soils) Project by the European Union's Horizon 2020 Programme for research & innovation under Grant Agreement number: 101000407.

Declarations

Competing interests

The authors declare no competing interests.

Additional information

Supplementary Information The online version contains supplementary material available at https://doi.org/10.1038/s41598-026-78484-4.

Correspondence and requests for materials should be addressed to M.B.

Reprints and permissions information is available at www.nature.com/reprints.

Publisher's note Springer Nature remains neutral with regard to jurisdictional claims in published maps and institutional affiliations.

Open Access This article is licensed under a Creative Commons Attribution 4.0 International License, which permits use, sharing, adaptation, distribution and reproduction in any medium or format, as long as you give appropriate credit to the original author(s) and the source, provide a link to the Creative Commons licence, and indicate if changes were made. The images or other third party material in this article are included in the article's Creative Commons licence, unless indicated otherwise in a credit line to the material. If material is not included in the article's Creative Commons licence and your intended use is not permitted by statutory regulation or exceeds the permitted use, you will need to obtain permission directly from the copyright holder. To view a copy of this licence, visit http://creativecommons.org/licenses/by/4.0/.

© The Author(s) 2026